DOI: 10.18721/JPM.13402

# TEMPERATURE EVOLUTION OF DIFFUSE SCATTERING IN THE STRONTIUM-BARIUM NIOBATE SBN-60 SINGLE CRYSTAL IN THE RELAXOR STATE

*P.Yu. Vanina*[1], *N.S. Silin*[1], *A.A. Bosak*[2], *D.Yu. Chernyshov*[1], *A.A. Naberezhnov*[3]

[1]Peter the Great St. Petersburg Polytechnic University, St. Petersburg, Russian Federation;

[2] European Synchrotron Radiation Facility, Grenoble, France;

[3] Ioffe Physical Technical Institute of the Russian Academy of Sciences, St. Petersburg, Russian Federation

Temperature dependences of synchrotron radiation diffuse scattering on the model relaxor single crystal $Sr_{0.6}Ba_{0.4}Nb_2O_6$ (SBN-60) have been studied in the temperature interval from 90 to 290 K in the vicinities of lattice points (332), (412) and (002) in the [001], [010] and [$1\bar{1}0$] directions. This diffuse scattering (DS) has been shown to be a strongly anisotropic with intensity $I_{DS}(T, q)$ proportional $q^{-\alpha}$ where $q$ is a reduce wavevector. The temperature dependences of the parameters α have been obtained, and it is established, that the microscopic modification of structure in the SBN-60 continues on cooling below the temperature of transition to the relaxor state.

**Keywords:** diffuse scattering, synchrotron radiation, relaxor, strontium-barium niobate, crystal structure

**Citation:** Vanina P.Y., Silin N.S., Bosak A.A., Chernyshov D.Y., Naberezhnov A.A., Temperature evolution of diffuse scattering in the strontium-barium niobate SBN-60 single crystal in the relaxor state, St. Petersburg State Polytechnical University Journal. Physics and Mathematics. 13 (4) (2020) 21–28. DOI: 10.18721/JPM.13402

This is an open access article under the CC BY-NC 4.0 license (https://creativecommons.org/licenses/by-nc/4.0/)

## Introduction

Solid solutions of strontium barium niobate (SBN) are model uniaxial ferroelectrics of the tungsten bronze family with a partially disordered structure. If the strontium content is $50\% < x < 75\%$, these $Sr_xBa_{1-x}Nb_2O_6$ solutions (SBN-$x$) exhibit distinct relaxor properties, which become more pronounced with increasing strontium concentration [1].

An SBN-$x$ structure is based on two types of $NbO_6$ octahedra, linked by oxygen atoms into a 3D network. This network includes three types of structural channels directed along the polar axis $c$ (along the [001] direction). Threefold channels are always empty in SBN-$x$, the medium-sized fourfold channels ($A_1$) are filled only with strontium atoms, the wide fivefold channels ($A_2$) are filled with barium and strontium atoms [2]. A characteristic peculiarity of the crystal structure of such compounds is that there are five divalent cations and one vacancy for six possible sites in $A_1$ and $A_2$ channels, which determines the statistical nature of the cation distribution [2].

Much attention is paid to solutions of the SBN-$x$ type, especially at $x \approx 60\%$, due to their relaxor, pyroelectric, dielectric, electro-optical and nonlinear optical properties [3–6]. Furthermore, it was found [7] that there is a critical strontium concentration in the range of 50–60%, above which normal ferroelectric domains do not exist: instead of them needle-like nanopolar domains are observed.

The SBN-60 crystal has a tetragonal structure with the following lattice parameters at room temperature:

$$a = b = 12.4566(9)\ \text{Å},\ c = 7.8698(6)\ \text{Å}.$$

We should also note that the SBN-60 structure is modulated, with the modulation vectors

$$\mathbf{q}_1 = 0.3075(6)\ (\mathbf{a}^* + \mathbf{b}^*),$$

$$\mathbf{q}_2 = 0.3075(6)\ (\mathbf{a}^* - \mathbf{b}^*),$$

where $\mathbf{a}^*$ and $\mathbf{b}^*$ are reciprocal lattice vectors.

The most adequate solution for the crystal structure of an SBN-61 single crystal (with a close concentration) is offered in [8], where it is described as an incommensurate structure in five-dimensional space within the superspace group $P4bm$ ($pp1/2$, $p$–$p1/2$).

Modulation of the structure was first observed in [9], and it was confirmed in [8] that it could be associated with the collective distortion of oxygen octahedra and the random occupation of 4*c* sites in the SBN structure with strontium and barium ions. Similar critical dynamics was also considered for an SBN-60 single crystal (similar in its structure and properties to SBN-61 doped with cerium). It has been established in [10–12] that transverse diffuse scattering (DS) by ferroelectric fluctuations is observed near the reciprocal lattice points of the (00L) type upon cooling from the high-temperature paraelectric phase, as the temperature of the transition to the relaxor state is approached; the DS intensity increases with decreasing temperatures, while the correlation length $r_c$ increases. DS consists of two components in the transition region; the first of these components is well described by the Lorentzian

$$G_1 \sim 1/(\kappa^2 + q^2),$$

and the second by the squared Lorentzian

$$G_2 \sim 1/(\kappa^2 + q^2)^2.$$

Here κ is the inverse correlation length ($r_c \sim 1/\kappa$), $q$ is the reduced wave vector.

Notably, the intensity of the second component increases sharply upon reaching the transition temperature. The dependence of the correlation length $r_c(T)$ on temperature has been obtained, and it has been found that this parameter 'freezes' below 340 K and remains practically constant up to 290 K [10]. Applying an external electric field suppresses both components of diffuse scattering, primarily, the component described by the function $G_2$ [10, 13].

On the other hand, the peculiarities of the crystal structure of SBN-60 (and its temperature evolution) on cooling in the relaxor phase are rather poorly understood at present: the only results available point to the existence of two different contributions to diffuse scattering [14]. Both types of scattering are considerably anisotropic: the first type is observed in the vicinity of superstructure reflections and is likely due to scattering by displacement waves in the system of oxygen octahedra, and the second is associated with the presence of local regions of correlated displacements of strontium and barium ions in fivefold SBN-60 channels.

This paper presents the first results on the temperature evolution of DS upon cooling from room temperature to 90 K.

## Experimental study

The measurements were carried out on the ID29 beamline at the European Synchrotron Radiation Facility (ESRF). The wavelength of incident radiation was $\lambda = 0.7749$ E, $\Delta\lambda/\lambda \approx 2\cdot10^{-4}$. The samples were needle-like crystals approximately 100 μm thick.

Two-dimensional distributions of the X-ray scattering intensity were obtained using a PILATUS 6M pixel detector [15]. Adjustment of the orientation matrix and preliminary reconstruction of the reciprocal space were carried out via the CrysAlis software package [16]. The measurements were taken on cooling in the temperature range from 290 to 90 K, temperature stability was maintained to within 1.5 K.

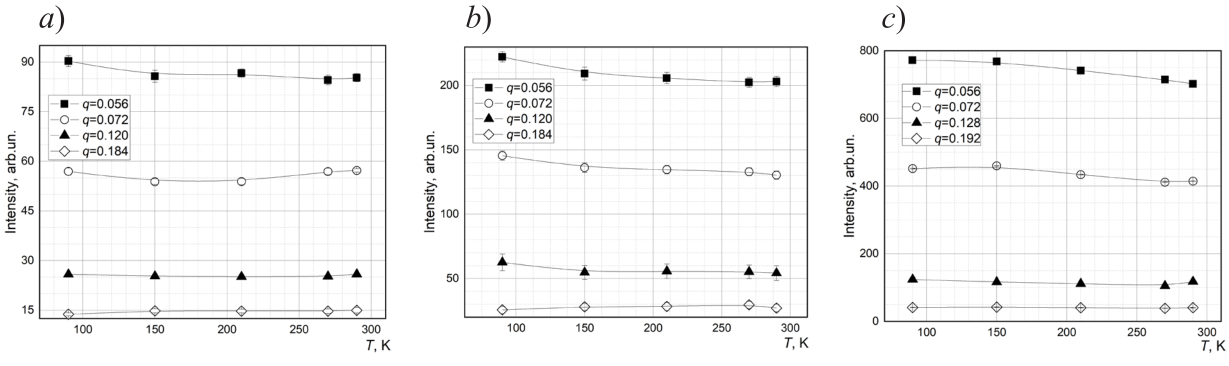


Fig. 1. Diffuse scattering intensities $I_{DS}(q,T)$ of synchrotron radiation as function of temperature in SBN-60 at different values of $q$ in the [001] direction in the vicinity of points (332) (*a*), (412) (*b*), (002) (*c*). The curves in the figures are the result of a smoothing procedure

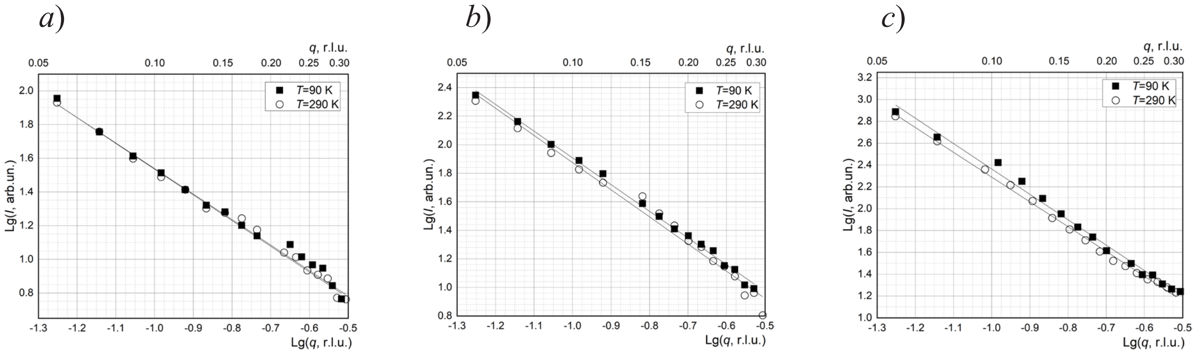


Fig. 2. DS intensities depending on the reduced wave vector (on a doubly logarithmic scale) in SBN-60 at 90 and 290 K in the [001] direction for points (332) (*a*), (412) (*b*), (002) (*c*). The values of $q$ are given in r.l.u. (reduced lattice units). The lines in the figures are the result of fitting

**Experimental results and discussion**

The temperature evolution of DS has been studied in the vicinity of reciprocal lattice points (002), (412) and (332) in three directions: [001], [010] and [1$\bar{1}$0] to obtain information on the potential anisotropy of diffuse scattering.

The dependence of the intensity $I$ from the reduced wave vector $q$ has been fitted by the following expression:

$$I(q) = I_{DS}(q) + I_{\mathrm{Br}}(q) + I_{bkg}(q). \quad (1)$$

The first term corresponds to diffuse scattering DS, which can be fitted to with the dependence $I_{DS}(q) \sim q^{-\alpha}$ at sufficiently large $q$ ($q > \kappa$). The second term $I_{\mathrm{Br}}(q)$ describes the Bragg contribution, and the third, $I_{bkg}(q)$, is the linear contribution of the background to the total scattering.

The elastic peak was described by a Gaussian; the exact position of the $q_c$ maximum was determined from the fit. The background was approximated by a linear function, the parameters were determined from averaging over 10–14 points, which were chosen to the left and right of $q_c$ at large $q$, when the contributions from both the elastic peak and the DS became negligible. With $|q| < 0.09$, the strong Bragg peak did not allow to reliably detect the weaker DS in all cases, while diffuse scattering at $|q| > 0.35$ could not be differentiated from the background.

Let us consider the behavior of the temperature dependences of DS intensity in the SBN-60 single crystal in the direction [001]. It is clear from Fig. 1 that the DS intensity is practically independent of temperature in this direction for all values of $q$.

Next, the dependences of the DS intensities on $q$ have been plotted for this direction on a doubly logarithmic scale in the entire investigated temperature range (Fig. 2). It is evident from the graphs that the relation $I_{DS}(q) \sim q^{-\alpha}$ is satisfied for all dependences $I_{DS}(q)$. The coefficients α corresponding to the slopes of the obtained straight lines are given in Table.

Table

**Values of parameter α for straight lines $\lg(I_{DS}) = -\alpha\lg(q) + b$, obtained at different temperatures for different directions and lattice points in SBN-60 single crystal (see Fig. 2)**

| Reciprocal lattice point | Direction in crystal | Value of parameter α | | | | |
|---|---|---|---|---|---|---|
| | | 90 K | 150 K | 210 K | 270 K | 290 K |
| (332) | [001] | 1.53(11) | 1.49(2) | 1.52(5) | 1.51(4) | 1.51(3) |
| | [010] | 3.52(10) | 3.47(9) | 3.45(7) | 3.18(4) | 2.89(10) |
| | [1$\bar{1}$0] | 3.48(6) | 3.49(4) | 3.50(5) | 3.36(5) | 2.87(5) |
| (412) | [001] | 1.87(3) | 1.81(4) | 1.86(6) | 1.81(5) | 1.85(6) |
| | [010] | 3.32(5) | 3.23(6) | 3.22(6) | 3.04(4) | 2.80(5) |
| | [1$\bar{1}$0] | 3.18(5) | 3.25(5) | 3.27(5) | 3.24(6) | 2.83(5) |
| (002) | [001] | 2.33(5) | 2.33(4) | 2.31(4) | 2.27(4) | 2.27(3) |
| | [010] | 3.20(5) | 3.15(5) | 3.11(5) | 2.87(5) | 2.57(3) |
| | [1$\bar{1}$0] | 2.76(1) | 2.68(2) | 2.57(2) | 2.24(4) | 1.92(4) |

We should note here that these parameters remain virtually unchanged over the entire temperature range considered for all reciprocal lattice points. In other words, diffuse scattering does not change upon cooling in the direction [001].

The temperature dependences of DS intensities of X-ray radiation in SBN-60, $I_{DS}(q,T)$, have been obtained by a similar procedure in the directions [010] and $[1\bar{1}0]$ for values of the reduced wave vector in the range of $0.112 < |q| < 0.288$ in the temperature range from 90 to 290 K (Fig. 3). It can be seen from the data in Fig. 3 that the diffuse scattering intensity $I_{DS}(q,T)$ increases upon cooling for all the given points at small $q$.

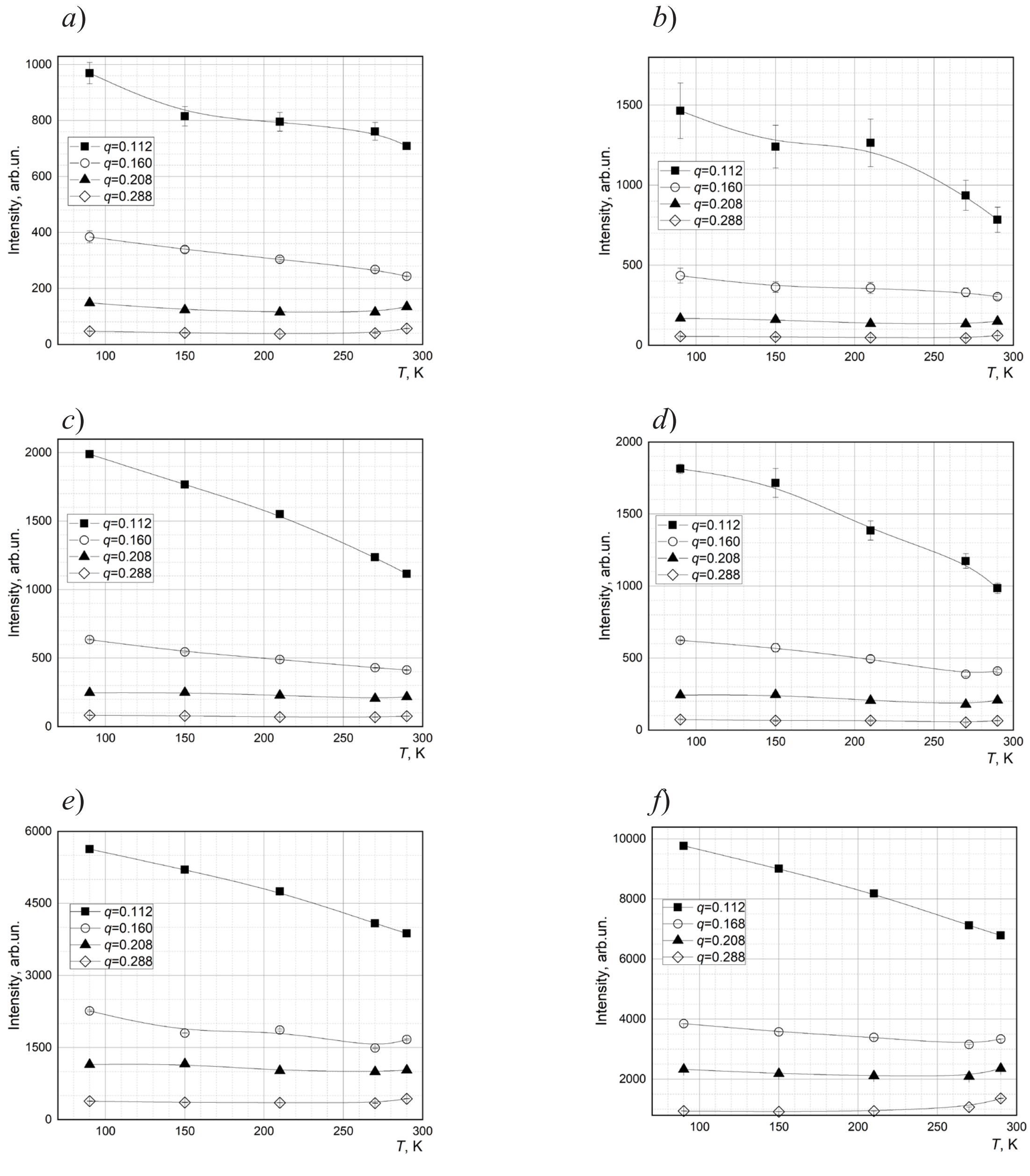


Fig. 3. Temperature dependences of DS intensities $I_{DS}(q,T)$ in SBN-60 single crystal at different values of $q$ in the vicinity of point (332) in the directions [010] (*a*), $[1\bar{1}0]$ (*b*), in the vicinity of point (412) in the directions [010] (*c*), $[1\bar{1}0]$ (*d*) and in the vicinity of point (002) in the directions [010] (*e*), $[1\bar{1}0]$ (*f*).
The curves in the figures are the result of a smoothing procedure

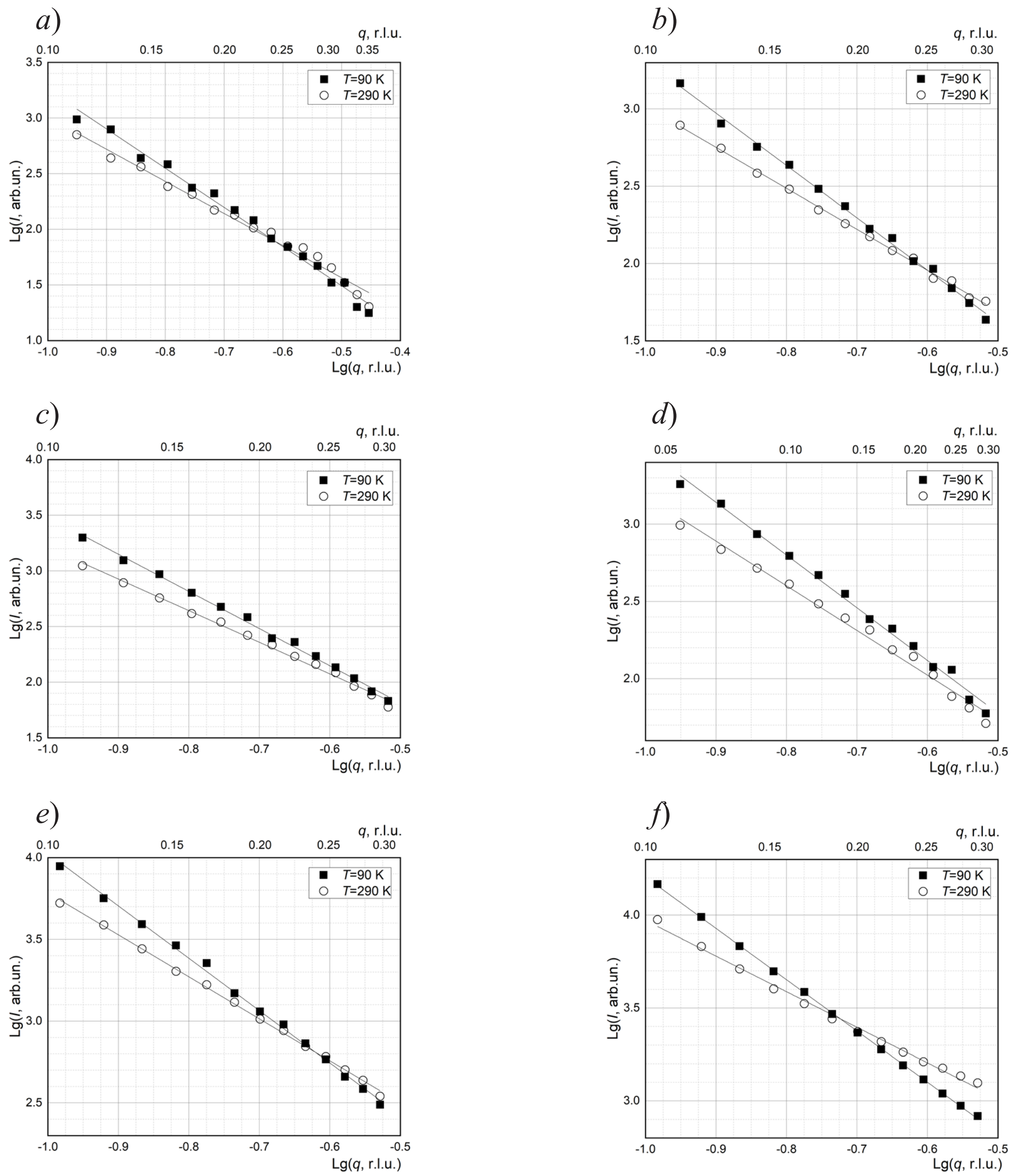


Fig. 4. DS intensities depending on the reduced wave vector (on a doubly logarithmic scale) in SBN-60 at 90 and 290 K in the vicinity of point (332) in the directions [010] (*a*) and $[1\bar{1}0]$ (*b*), in the vicinity of point (412) in the directions [010] (*c*) and $[1\bar{1}0]$ (*d*), in the vicinity of point (002) in the directions [010] (*e*) &$[1\bar{1}0]$ (*f*). The values of $q$ are given in r.l.u. The lines in the figures are the result of fitting

Next, the dependences of DS intensities on the reduced wave vector $q$ have been plotted on a doubly logarithmic scale for the entire temperature range of 90–290 K (see Table). In Fig. 4, the dependences $I_{DS}(q)$ at 290 and 90 K are presented for comparison. Apparently, the linear character of the obtained dependences is clearly observed in these cases, i.e., there is a power-law dependence of the intensity DS in the vicinity of these point: $I_{DS}(q) \sim q^{-\alpha}$. Notably, the parameters α characterizing the slope of the curves increase significantly on cooling, reaching the following values: 3.52 and 3.48 for point (332) in the directions [010] and $[1\bar{1}0]$, respectively; 3.32 and 3.18 for point (412), and 3.20 and 2.76 for point (002) at $T = 90$ K (see Table).

Thus, analysis of the data obtained points to the existence of two contributions to diffuse scattering:

DS-1, which increases with decreasing temperature along the directions [010] and $[1\bar{1}0]$, with the parameter α increasing as well;

DS-2, which is practically independent of temperature along the direction [001] in the entire range of 90–290 K, the same as the parameter α; however, the values of the parameter α differ in the vicinity of different reciprocal lattice points.

Importantly, the obtained temperature dependences of the DS-1 and DS-2 intensities give reason to believe that neither type of scattering is thermal diffuse one (TDS), for which the intensity should increase on heating [17].

As mentioned above, it has been found in [10] that an additional contribution from the squared Lorentzian $G_2$ appears upon cooling from the paraelectric phase along with the contribution described by the Lorentzian $G_1$, which is typical for critical scattering; this contribution increases at transition to the relaxor phase. As a result, the total diffuse scattering is described by the superposition of the functions $G_1$ and $G_2$, and at sufficiently large values of $q$ ($q > \kappa$) the experimental value of α in the scattering law $q^{-\alpha}$ exceeds 2. We also observe the same effect in this case for DS-1 at temperature decreasing, and the growth of α upon cooling indicates an increase of $G_2$ contribution into DS-1. In a sense, similar behavior of the parameter α has been observed in [18] for the lithium doped $KTaO_3$ single crystal (1.6% Li) below $T_C$ (the phase transition temperature is about 35 K).

The function $G_1$ corresponds in direct space (in the isotropic three-dimensional case) to a correlation function of the form

$$C_1 = \exp(-\kappa r)/r,$$

characterized by the presence of a ‘cut-off’ factor $1/r$, that is, such a correlator is characteristic of regions of local ordering (correlation) with rather sharp boundaries.

The functions $G_2$ corresponds in direct space to a correlator of the form

$$C_2 = \exp(-\kappa r),$$

containing no ‘cut-off’ factor, i.e., such a correlation function is typical for regions with smeared boundaries.

Thus, it can be concluded from the observed growths of the DS-1 intensity and the slope parameter α upon cooling that local rearrangement of the structure continues in SBN-60 as the temperature decreases (at least down to 90 K), with an increase in the contribution from regions with blurred boundaries, which is what contributes to an increase in α. In turn, a growth of the DS-1 intensity upon cooling indicates an increase in the ‘density’ (i.e., the total number) of such regions.

The approaches for interpreting the data on small-angle neutron and X-ray scattering (SANS and SAXS) can be used to explain the absence of temperature dependences of both the DS-2 intensity and the slope parameters α in this case. It is known that in the case of a mass fractal with the fractal dimension $D$ for parameter α in the scattering law $I(q) \sim q^{-\alpha}$ (I is the intensity, q is the transferred momentum) the relation $D = \alpha$, where $1 < \alpha < 3$, holds true [19–21]. For example, $\alpha = 1$ for a one-dimensional chain of mass spheres, and $1 \le D \le 3$, where $D$ is a non-integer, for aggregates constructed from spheres without overlapping. The parameter $D$ corresponds to the distribution of mass in space. This approach offers a logical explanation for the experimental values obtained for the parameter α, if, for example, the corresponding agglomerates of atomic chains in SBN-60 are regarded as scattering objects.

## Conclusion

We have considered the temperature dependences for diffuse scattering intensity of synchrotron radiation, $I_{DS}(T,q)$ ($q$ is the reduced wave vector), in a single crystal of strontium-barium niobate $Sr_{0.6}Ba_{0.4}Nb_2O_6$ in the vicinity of the crystal lattice points (332), (412) and (002), in three fundamental directions: [001], [010], [$1\bar{1}0$].

It has been established that the $I_{DS}(T,q)$ dependences are well described by the power law $q^{-\alpha}$ on a doubly logarithmic scale; the temperature dependences of the parameters α have been obtained.

We have found that diffuse scattering is substantially anisotropic in the vicinity of the given points and consists of two components (DS-1 and DS-2) with fundamentally different behavior both the temperature dependences of the intensities and the parameters α.

The intensity of the DS-1 component and the corresponding parameter α increase at temperature decreasing, which indicates that the evolution of the local structure in SBN-60, associated with the smearing of the boundaries of the regions of local ordering, continues on cooling.

As for the behavior of the DS-2 component observed in the [001] direction, neither the intensity nor the parameter α depend on temperature in the range considered (90–290 K), but the value of α depends on the reciprocal lattice point in whose vicinity the measurements have been taken. It is likely that the nature of DS-2 is associated with scattering by mass fractal structures.

The study was carried out at Peter the Great St. Petersburg Polytechnic University within the framework of a State Task for Basic Research (topic code 0784-2020-0025). D.Yu. Chernyshev expresses his gratitude to the Russian Foundation for Basic Research for partial financial support of the studies on this subject (grant no. 19-29-12023).

The authors declare no conflict of interest.

## REFERENCES


1. **Viehland D., Xu Z., Huang W.-H.,** Structure-property relationships in strontium barium niobate. I. Needle-like nanopolar domains and the metastably-locked incommensurate structure, Philos. Mag. A. 1995. Vol. 71 (2) (1995) 205–217.

2. **Chernaya T.S., Maksimov B.A., Verin I.A., et al.,** Crystal structure of $Ba_{0.39}Sr_{0.61}Nb_2O_6$ single crystals, Crystallography Reports. 42 (3) (1997) 375–380.

3. **Glass A.M.,** Investigation of the electrical properties of $Sr_{1-x}Ba_xNb_2O_6$ with special reference to pyroelectric detection, J. Appl. Phys. 40 (12) (1969) 4699–4713.

4. **Ewbank M.D., Neurgaonkar R.R., Cory W.K., Feinberg J.,** Photorefractive properties of strontium-barium niobate, J. Appl. Phys. 1987. Vol. 62 (2) (1987) 374–380.

5. **Romero, J.J., Aragy C., Gonzalo J.A., et al.,** Spectral and thermal properties of quasiphase-matching second-harmonic-generation in $Nd^{3+}$: $Sr_{0.6}Ba_{0.4}(NbO_3)_2$ multiself-frequency-converter nonlinear crystals, J. Appl. Phys. 93 (5) (2003) 3111–3113.

6. **Simagina L.V., Mishina E.D., Semin S.V., et al.,** Second harmonic generation in microdomain gratings fabricated in strontium-barium niobate crystals with an atomic force microscope, J. Appl. Phys. 110 (5) (2011) 052015–052020

7. **Kuz`minov Yu.S.,** Segnetoelektricheskie kristally dlya upravleniya lazernym izlucheniem [Ferroelectric crystals to control laser emission], Nauka, Moscow, 1982 (in Russian).

8. **Woike T., Petricek V., Dusek M., et al.,** The modulated structure of $Ba_{0.39}Sr_{0.61}Nb_2O_6$. I. Harmonic solution, Acta Crystallographica, Section B. 59 (Part 1, February) (2003) 28–35.

9. **Schneck J., Toledano J.C., Whatmore F, Ainger F.W.,** Incommensurate phases in ferroelectric tetragonal tungsten bronzes, Ferroelectrics. 36 () (1981) 327–330.

10. **Borisov S.A., Okuneva N.M., Vakhrushev S.B., et al.,** Critical neutron scattering in a uniaxial relaxor $Sr_{0.6}Ba_{0.4}Nb_2O_6$, Physics of the Solid State. 55 (2) (2013) 334–341.

11. **Chillal S., Koulialias D., Gvasaliya S.N., et al.,** Phase transition of chemically doped uniaxial relaxor ferroelectric, J. Phys.: Condens. Matter. 27 (43) (2015) 435901 (8p.).

12. **Ondrejkovic P., Kempa M., Kulda J., et al.,** Dynamics of nanoscale polarization fluctuations in a uniaxial relaxor, Phys. Rev. Lett. 113 (16) (2014) 167601.

13. **Ondrejkovic P., Kempa M., Savinov M., et al.,** Electric-field influence on the neutron diffuse scattering near the ferroelectric transition of $Sr_{0.61}Ba_{0.39}Nb_2O_6$, Phase Transit. 89 (7–8) (2016) 808–816.

14. **Vanina P.Yu, Vakhrushev S.B., Naberezhnov A.A., Bosak A.A.,** Multiscale local ordering in the prototypical uniaxial relaxor $Sr_{0.6}Ba_{0.4}Nb_2O_6$ single crystal at room temperature, J. Phys.: Condens. Matter. 31 (No. 17) (2019) 175401.

15. **Brųnnimann C., Eikenberry E.F., Henrich B., et al.,** The PILATUS 1M detector, J. Synchrotron. Radiat. 13 (Part 2, March) (2006) 120–130.

16. Agilent, CrysAlis PRO, Agilent Technologies, Yarnton, Oxfordshire, England, 2011.

17. **Willis B.T.M., Pryor A.W.,** Thermal vibrations in crystallography, Cambridge University Press, Cambridge, 1975.

18. **Andrews S.R.,** X-ray scattering study of the random electric dipole system $KTaO_3$: Li, J. Phys. C. Solid State Phys. 18 (7) (1985) 1357–1376.

19. **Jullien R.,** Fractal aggregates, Comm. Cond. Mat. Phys. (Comm. Mod. Phys. Pt. B). 13 (4) (1987) 177–205.

20. **Avdeev M.V., Aksenov V.L.,** Small-angle neutron scattering in structure research of magnetic fluids, Physics Uspekhi. 53 (10) (2010) 971–993.

21. **Cousin F.,** Small angle neutron scattering, EPJ Web of Conferences. 104 (2015) 01004 (1–49).


*Received 05.09.2020, accepted 10.09.2020.*

## THE AUTHORS

**VANINA Polina Yu.**
*Peter the Great St. Petersburg Polytechnic University*
29 Politechnicheskaya St., St. Petersburg, 195251, Russian Federation
p.yu.vanina@gmail.com

**SILIN Nikita S.**
*Peter the Great St. Petersburg Polytechnic University*
29 Politechnicheskaya St., St. Petersburg, 195251, Russian Federation
silin.ns@edu.spbstu.ru

**BOSAK Alexey A.**
*European Synchrotron Radiation Facility*
71, Avenue des Martyrs, Grenoble, 38000, France
alexei.bossak@esrf.fr

**CHERNYSHOV Dmitry Yu.**
*Peter the Great St. Petersburg Polytechnic University*
29 Politechnicheskaya St., St. Petersburg, 195251, Russian Federation
chernyshov65@gmail.com

**NABEREZHNOV Alexander A.**
*Ioffe Physical Technical Institute of the Russian Academy of Sciences*
26 Polytekhnicheskaya St., St. Petersburg, 194021, Russian Federation
alex.nabereznov@mail.ioffe.ru

© Peter the Great St. Petersburg Polytechnic University, 2020